

UNSTEADY FLOW AND HEAT TRANSFER OF JEFFREY FLUID OVER A STRETCHING SHEET

by

**Tasawar HAYAT^{a,b}, Zahid IQBAL^{a*}, Meraj MUSTAFA^c,
and Ahmed ALSAEDI^b**

^a Department of Mathematics, Quaid-I-Azam University, Islamabad, Pakistan

^b Department of Mathematics, Faculty of Science, King Abdulaziz University, Jeddah, Saudi Arabia

^c Research Centre for Modeling and Simulation, National University of Sciences and
Technology, Islamabad, Pakistan

Original scientific paper
DOI: 10.2298/TSCI110907092H

The boundary layer flow and heat transfer of an incompressible Jeffrey fluid have been investigated. The analytic solutions of the arising differential system have been computed by homotopy analysis method. The dimensionless expressions for wall shear stress and surface heat transfer are also derived. Exact solutions of the momentum equation and numerical solutions of the dimensionless energy equations have been obtained for the steady-state case. The results indicate an increase in the velocity and the boundary layer thickness by increasing the elastic parameter (Deborah number) for a Jeffrey fluid.

Key words: *unsteady flow, heat transfer, analytic solution, viscous dissipation*

Introduction

Interest in the boundary layer flows of non-Newtonian fluids has increased due to the applications in science and engineering including thermal oil recovery, food and slurry transportation, polymer and food processing, *etc.* A variety of non-Newtonian fluid models have been proposed in the literature keeping in view of their several rheological features. In these fluids, the constitutive relationships between stress and rate of strain are much complicated in comparison to the Navier-Stokes equations. There is one subclass of non-Newtonian fluids known as Jeffrey fluid [1-4] which has been attracted much by the researchers in view of its simplicity. This fluid model is capable of describing the characteristics of relaxation and retardation times.

Heat transfer in the flows induced by the stretching surfaces has several applications. In fact the production of sheeting material is involved in various manufacturing processes and includes both metal and polymer sheets.

The rate of heat transfer over a surface has a pivotal role in the quality of final product. Industrial applications include fibers spinning, hot rolling, manufacturing of plastic and rubber sheet, continuous casting and glass blowing. Crane [5] studied the boundary layer flow of an incompressible viscous fluid towards a linear stretching sheet. An exact similarity solution for the

* Corresponding author; e-mail: zahidiqbal_qau@yahoo.com

dimensionless differential system was obtained. Such closed form similarity solution has been obtained for several other features like viscoelasticity, magnetohydrodynamics, suction, porosity, and heat and mass transfer [6, 7, 8, 9]. Andersson *et al.* [10] discussed the slip effects on the flow of a viscous fluid over a stretching sheet. Axisymmetric flow of viscous fluid over a stretching sheet has been examined by Ariel [11]. Analytic solutions valid for large and small values of slip parameter have been obtained. Abbas and Hayat [12] provided an analytic solution for stagnation slip flow and heat transfer towards a stretching sheet by homotopy analysis method (HAM). Combined effects of slip and heat transfer on the flow of viscoelastic fluid were analyzed by Hayat *et al.* [13]. A homotopy solution valid for all values of slip parameter was obtained. Effect of suction on the 2-D and axisymmetric flows in the presence of partial slip has been examined by Wang [14]. Liao [15] presented the analytic solution for magnetohydrodynamic boundary layer flow of a power-law fluid towards a stretching surface. Dimensionless expressions for skin friction coefficient have been thoroughly addressed. A literature survey reveals significant research has been conducted on the steady boundary layer flows. However the time-dependent boundary layer flows have been scarcely studied. Devi *et al.* [16] numerically investigated the unsteady mixed convection stagnation-point flow towards a stretching surface. Andersson *et al.* [17] examined the heat transfer characteristics on the flow induced by an unsteady stretching sheet. Nazar *et al.* [18] discussed the unsteady boundary layer rotating flow due to a stretching surface. Liao [19] performed an analytic treatment of the unsteady boundary layer flow of a viscous fluid over a stretching surface. Mukhopadhyay [20] examined the effect of thermal radiation on the unsteady mixed convection flow and heat transfer bounded by a porous stretching surface embedded in a porous medium.

The present work deals with the analysis of unsteady boundary layer flow and heat transfer of Jeffrey fluid. Following Crane [5], an exact solution for the dimensionless momentum equation has been obtained for the steady-state case. However the energy equation has been solved numerically by MATHEMATICA. HAM has been employed to obtain the analytic solutions for all the dimensionless time ($0 \leq \tau \leq \infty$) in the whole spatial domain ($0 \leq \eta \leq \infty$). This method has been successfully applied to various interesting problems [21-30]. Graphs are portrayed to gain physical insight towards the embedding physical parameters.

Mathematical model

We consider the unsteady incompressible flow of a Jeffrey fluid past a stretching sheet situated at $y = 0$. The x - and y -axes are taken along and perpendicular to the sheet, respectively, and the flow is confined to $y \geq 0$. It is assumed that the velocity of the stretching sheet is $u_w(x) = ax$, where a is a positive (stretching sheet) constant. The viscous dissipation effects are retained. The boundary layer equations governing the unsteady flow and heat transfer of a Jeffrey fluid are:

$$\frac{\partial u}{\partial x} + \frac{\partial v}{\partial y} = 0 \quad (1)$$

$$\begin{aligned} & \frac{\partial u}{\partial t} + u \frac{\partial u}{\partial x} + v \frac{\partial u}{\partial y} = \\ & = \frac{\nu}{1 + \lambda_2} \left[\frac{\partial^2 u}{\partial y^2} + \lambda_1 \left(\frac{\partial^3 u}{\partial y^2 \partial t} + u \frac{\partial^3 u}{\partial x \partial y^2} - \frac{\partial u}{\partial x} \frac{\partial^2 u}{\partial y^2} + \frac{\partial u}{\partial y} \frac{\partial^2 u}{\partial x \partial y} + v \frac{\partial^3 u}{\partial y^3} \right) \right] \end{aligned} \quad (2)$$

$$\frac{\partial T}{\partial t} + u \frac{\partial T}{\partial x} + v \frac{\partial T}{\partial y} = \alpha \frac{\partial^2 T}{\partial y^2} + \frac{v}{C_p(1+\lambda_2)} \left[\left(\frac{\partial u}{\partial y} \right)^2 + \lambda_1 \left(u \frac{\partial u}{\partial y} \frac{\partial^2 u}{\partial x \partial y} + \frac{\partial u}{\partial y} \frac{\partial^2 u}{\partial t \partial y} + v \frac{\partial u}{\partial y} \frac{\partial^2 u}{\partial y^2} \right) \right] \quad (3)$$

The boundary conditions are:

$$\begin{aligned} t < 0: \quad v = 0, \quad u = 0, \quad T = T_\infty \quad \text{for any } x \text{ and } y \\ t \geq 0: \quad u = ax, \quad v = 0, \quad T = T_w \quad \text{at } y = 0, \\ u \rightarrow 0, \quad T \rightarrow T_\infty, \quad \text{as } y \rightarrow \infty \end{aligned} \quad (4)$$

in which u and v are the velocity components along x - and y -directions, respectively, ρ – the fluid density, $\nu = \mu/\rho$ – the kinematic viscosity, T – the fluid temperature, α – the thermal diffusivity, C_p – the specific heat, λ_2 – the ratio of relaxation and retardation time, and λ_1 – the relaxation time. Introducing [5]:

$$\begin{aligned} \eta = \sqrt{\frac{a}{\nu \xi}} y, \quad u = axf'(\eta, \xi), \quad v = -\sqrt{av\xi} f(\eta, \xi), \\ \xi = 1 - \exp[-\tau], \quad \tau = at, \quad \theta(\eta, \xi) = \frac{T - T_\infty}{T_w - T_\infty} \end{aligned} \quad (5)$$

Equation (1) is automatically satisfied and eqs. (2)-(4) can be written as:

$$\begin{aligned} [\xi - \beta(1-\xi)]f''' + (1+\lambda_2) \left[\xi(1-\xi) \left(\frac{\eta}{2} f'' - \xi \frac{\partial f'}{\partial \xi} \right) - \xi^2 (f'^2 - ff'') \right] + \\ + \beta \left[\xi(1-\xi) \frac{\partial f''}{\partial \xi} - \frac{\eta}{2} (1-\xi) f^{iv} + \xi (f'^2 - ff'') \right] = 0 \end{aligned} \quad (6)$$

$$\begin{aligned} \xi \theta'' + \text{Pr} \xi (1-\xi) \left(\frac{\eta}{2} \theta' - \xi \frac{\partial \theta}{\partial \xi} \right) + \text{Pr} \xi^2 f \theta' \frac{\text{Pr Ec}}{1+\lambda_2} \left\{ \xi - \frac{\beta(1-\xi)}{\xi} \right\} f'^2 + \\ + \frac{\text{Pr Ec} \beta}{1+\lambda_2} \left[\xi (ff''^2 - ff''') + (1-\xi) \left(\xi f'' \frac{\partial f''}{\partial \xi} - \frac{\eta}{2} f f''' \right) \right] = 0 \end{aligned} \quad (7)$$

$$f(0, \xi) = 0, \quad f'(0, \xi) = 1, \quad \theta(0, \xi) = 1, \quad f'(\infty, \xi) = 0, \quad \theta(\infty, \xi) = 0 \quad (8)$$

where Pr is the Prandtl number, Ec – the Eckert number and β – the Deborah number which are defined by:

$$\text{Pr} = \frac{\nu}{\alpha}, \quad \beta = a\lambda_1, \quad \text{Ec} = \frac{(u_w)^2}{C_p(T_w - T_\infty)} \quad (9)$$

It is worth mentioning here that $\text{Ec} > 0$ corresponds to the heated wall ($T_w > T_\infty$) and corresponds to the case when the viscous dissipation term in the energy eq. (3) is neglected.

The skin friction coefficient C_f and local Nusselt number Nu_x are:

$$C_f = \frac{\tau_w}{\rho u_w^2}, \quad \text{Nu}_x = \frac{xq_w}{k(T_w - T_\infty)} \quad (10)$$

where the wall skin friction τ_w and the heat transfer q_w from the plate are given by:

$$\tau_w = \frac{\mu}{1 + \lambda_2} \left[\frac{\partial u}{\partial y} + \lambda_1 \left(\frac{\partial^2 u}{\partial y \partial t} + u \frac{\partial^2 u}{\partial y \partial x} + v \frac{\partial^2 u}{\partial y^2} \right) \right]_{y=0} \quad (11)$$

$$q_w = -k \left(\frac{\partial T}{\partial y} \right)_{y=0} \quad (12)$$

In view of eq. (5), the above expressions give:

$$\sqrt{\xi} \sqrt{\text{Re}_x} C_f = \frac{1}{1 + \lambda_2} \left\{ (1 + \beta) f''(0, \xi) - \beta(1 - \xi) \left[\frac{\partial f''(0, \xi)}{\partial \xi} - \frac{1}{2\xi} f''(0, \xi) \right] \right\} \quad (13)$$

$$\frac{1}{\sqrt{\xi}} \frac{1}{\sqrt{\text{Re}_x}} \text{Nu}_x = -\theta'(0, \xi) \quad (14)$$

where $\text{Re}_x = u_w x / \nu$ is the local Reynolds number.

Steady-state flow ($\zeta = 1$)

This solution corresponds to $\xi = 1$, where $f_s(\eta, 1)$ and $\theta(\eta, 1) = \theta_s(\eta)$. In this case eqs. (6)-(8) reduce to:

$$f_s''' + (1 + \lambda_2)(-f_s'^2 + f_s f_s'') + \beta(f_s''^2 - f_s f_s^{iv}) = 0, \quad (15)$$

$$(1 + \lambda_2)(\theta_s'' + \text{Pr} f_s \theta_s') + \text{Pr} \text{Ec} [f_s''^2 + \beta(f_2' f_s''^2 - f_s f_s'' f_s''')] = 0 \quad (16)$$

$$f_s(0) = 0, \quad f_s'(0) = 1, \quad \theta_s(0) = 1, \quad f_s'(\infty) = 0, \quad \theta_s(\infty) = 0 \quad (17)$$

It is important to note that exact solution of eq. (15) subject to boundary conditions (17) has the form:

$$f_s(\eta) = \frac{1 - e^{-m\eta}}{m}; \quad m = \sqrt{\frac{1 + \lambda_2}{1 + \beta}} \quad (18)$$

After substituting the expression of f_s from eq. (18) in eq. (16) we have solved the resulting differential equation numerically by a symbolic computation software MATHEMATICA.

Computations by homotopy analysis method (HAM)

Zeroth-order deformation problems

We select the initial guesses and the linear operator as:

$$f_0(\eta, \xi) = 1 - e^{-\eta}, \quad \theta_0(\eta, \xi) = e^{-\eta} \quad (19)$$

$$L_f(f) = f''' - f' \quad (20)$$

$$L_\theta(f) = f'' - f \quad (21)$$

where L_f and L_θ satisfy the following properties:

$$L_f(A_1 + A_2 e^\eta + A_3 e^{-\eta}) = 0 \quad (22)$$

$$L_\theta(A_4 e^\eta + A_5 e^{-\eta}) = 0 \quad (23)$$

where $A_i (i = 1-5)$ are the arbitrary constants and the non-linear operators N_f and N_θ are:

$$N_f[\bar{f}(\eta, \xi; p)] = [\xi - \beta(1 - \xi)] \frac{\partial^3 \bar{f}(\eta, \xi; p)}{\partial \eta^3} + (1 + \lambda_2) \cdot \left\{ \begin{aligned} &\xi^2 \left[\left(\frac{\partial \bar{f}(\eta, \xi; p)}{\partial \eta} \right)^2 - \bar{f}(\eta, \xi) \frac{\partial^2 \bar{f}(\eta, \xi; p)}{\partial \eta^2} \right] + \\ &+ (1 - \xi) \left(\frac{\eta}{2} \xi \frac{\partial^2 \bar{f}(\eta, \xi; p)}{\partial \eta^2} - \xi^2 \frac{\partial^2 \bar{f}(\eta, \xi; p)}{\partial \eta \partial \xi} \right) \end{aligned} \right\} + \beta \left\{ (1 - \xi) \left[\xi \frac{\partial^4 \bar{f}(\eta, \xi; p)}{\partial \eta^3 \partial \xi} - \frac{\eta}{2} \frac{\partial^4 \bar{f}(\eta, \xi; p)}{\partial \eta^4} \right] + \xi \left[\begin{aligned} &\left(\frac{\partial^2 \bar{f}(\eta, \xi; p)}{\partial \eta^2} \right)^2 - \\ &- \bar{f}(\eta, \xi; p) \frac{\partial^3 \bar{f}(\eta, \xi; p)}{\partial \eta^3} \end{aligned} \right] \right\} \quad (24)$$

$$N_\theta[\bar{\theta}(\xi, \eta; p), \bar{f}(\xi, \eta; p)] = \xi \frac{\partial^2 \bar{\theta}(\xi, \eta; p)}{\partial \eta^2} + \text{Pr} \xi (1 - \xi) \left(\frac{\eta}{2} \frac{\partial \bar{\theta}(\xi, \eta; p)}{\partial \eta} - \xi \frac{\partial \bar{\theta}(\xi, \eta; p)}{\partial \xi} \right) + \text{Pr} \xi \bar{f}(\xi, \eta; p) \frac{\partial \bar{\theta}(\xi, \eta; p)}{\partial \eta} + \frac{\text{Pr Ec}}{1 + \lambda_2} \left[\xi - \frac{\beta(1 - \xi)}{\xi} \right] \left[\frac{\partial^2 \bar{f}(\xi, \eta; p)}{\partial \eta^2} \right]^2 + \frac{\text{Pr Ec} \beta}{(1 + \lambda_2)} \left\{ \begin{aligned} &\xi \left[\frac{\partial \bar{f}(\eta, \xi; p)}{\partial \eta} \left(\frac{\partial^2 \bar{f}(\eta, \xi; p)}{\partial \eta^2} \right)^2 - \frac{\partial \bar{f}(\eta, \xi; p)}{\partial \eta} \frac{\partial^2 \bar{f}(\eta, \xi; p)}{\partial \eta^2} \frac{\partial^3 \bar{f}(\eta, \xi; p)}{\partial \eta^3} \right] + \\ &+ (1 - \xi) \left[\xi \frac{\partial^2 \bar{f}(\eta, \xi; p)}{\partial \eta^2} \frac{\partial^3 \bar{f}(\eta, \xi; p)}{\partial \eta^2 \partial \xi} - \frac{\eta}{2} \frac{\partial^2 \bar{f}(\eta, \xi; p)}{\partial \eta^2} \frac{\partial^3 \bar{f}(\eta, \xi; p)}{\partial \eta^3} \right] \end{aligned} \right\} \quad (25)$$

The problems at the zeroth order are:

$$(1 - p)L_f[\bar{f}(\eta, \xi; p) - f_0(\eta, \xi)] = ph_f N_f[\bar{f}(\eta, \xi; p)] \quad (26)$$

$$(1 - p)L_\theta[\bar{\theta}(\eta, \xi; p) - \theta_0(\eta, \xi)] = ph_\theta N_\theta[\bar{f}(\eta, \xi; p), \bar{\theta}(\eta, \xi; p)] \quad (27)$$

$$\bar{f}(0, \xi; p) = 0, \quad \bar{f}'(0, \xi; p) = 1, \quad \bar{\theta}(0, \xi; p) = 1, \quad \bar{f}(\infty, \xi; p) = 0, \quad \bar{\theta}(\infty, \xi; p) = 0 \quad (28)$$

In the above equations h_f and h_θ are auxiliary non-zero parameters and $p \in [0, 1]$ is an embedding parameter. For $p = 0$ and $p = 1$, one has:

$$\bar{f}(\eta, \xi; 0) = f_0(\eta, \xi), \quad \bar{f}(\eta, \xi; 1) = f(\eta, \xi), \quad (29)$$

$$\bar{\theta}(\eta, \xi; 0) = \theta_0(\eta, \xi), \quad \bar{\theta}(\eta, \xi; 1) = \theta(\eta, \xi) \quad (30)$$

When p increases from 0 to 1, $\bar{f}(\eta, \xi; p)$ and $\bar{\theta}(\eta, \xi; p)$ vary continuously from the initial guesses $f_0(\eta, \xi)$ and $\theta_0(\eta, \xi)$ to the final solutions $f(\eta, \xi)$ and $\theta(\eta, \xi)$. By Taylor's theorem and eqs. (29) and (30) we get:

$$\bar{f}(\eta, \xi; p) = f_0(\eta, \xi) + \sum_{m=1}^{\infty} f_m(\eta, \xi) p^m; \quad f_m(\eta, \xi) = \frac{1}{m!} \left. \frac{\partial^m \bar{f}(\eta, \xi; p)}{\partial p^m} \right|_{p=0} \quad (31)$$

$$\bar{\theta}(\eta, \xi; p) = \theta_0(\eta, \xi) + \sum_{m=1}^{\infty} \theta_m(\eta, \xi) p^m; \quad \theta_m(\eta, \xi) = \frac{1}{m!} \left. \frac{\partial^m \bar{\theta}(\eta, \xi; p)}{\partial p^m} \right|_{p=0} \quad (32)$$

The auxiliary parameters h_f and h_θ are so properly selected such that series solutions converge at $p = 1$. Substituting $p = 1$, one obtains:

$$f(\eta, \xi) = f_0(\eta, \xi) + \sum_{m=1}^{\infty} f_m(\eta, \xi) \quad (33)$$

$$\theta(\eta, \xi) = \theta_0(\eta, \xi) + \sum_{m=1}^{\infty} \theta_m(\eta, \xi) \quad (34)$$

m^{th} -order deformation problems

The problems at this order are:

$$L_f[f_m(\eta, \xi, p) - \chi_m f_{m-1}(\eta, \xi)] = h_f R_{1,m}(\eta, \xi) \quad (35)$$

$$L_\theta[\theta_m(\eta, \xi, p) - \chi_m \theta_{m-1}(\eta, \xi)] = h_\theta R_{2,m}(\eta, \xi) \quad (36)$$

$$f_m(0, \xi) = f'_m(0, \xi) = f'_m(\infty, \xi) = \theta_m(0, \xi) = \theta_m(\infty, \xi) = 0 \quad (37)$$

$$R_{1,m}(\eta, \xi) = [\xi - \beta(1 - \xi)]f'''_{m-1} + (1 + \lambda_2)(1 - \xi) \left(\frac{\eta}{2} \xi f''_{m-1} - \xi^2 \frac{\partial f'_{m-1}}{\partial \xi} \right) + \\ + \beta(1 - \xi) \left(-\frac{\eta}{2} f'_{m-1} + \xi \frac{\partial f''_{m-1}}{\partial \xi} \right) + \\ + \sum_{k=0}^{m-1} \{ (1 + \lambda_2)(\xi^2 f_{m-1-k} f''_k - \xi^2 f'_{m-1-k} f'_k) + \beta \xi (-f_{m-1-k} f'_k + f'_{m-1-k} f''_k) \} \quad (38)$$

$$R_{2,m}(\eta, \xi) = \xi \theta''_{m-1} - \text{Pr}(1 - \xi) \left(\frac{\eta}{2} \theta'_{m-1} - \xi \frac{\partial \theta_{m-1}}{\partial \xi} \right) + \xi^2 \text{Pr} \sum_{k=0}^{m-1} [f_k \theta'_{m-1-k}] + \\ + \frac{\text{Pr Ec}}{1 + \lambda_2} \left[\xi - \frac{\beta(1 - \xi)}{\xi} \right] \sum_{k=0}^{m-1} f''_{m-1-k} f''_k + \\ + \frac{\text{Pr Ec} \beta}{1 + \lambda_2} \left[\xi \sum_{k=0}^{m-1} \sum_{l=0}^k f'_{m-1-k} f''_{k-l} f'_l - \xi \sum_{k=0}^{m-1} \sum_{l=0}^k f_{m-1-k} f''_{k-l} f'_l \right] + \\ + \frac{\text{Pr Ec} \beta}{1 + \lambda_2} \left[\xi(1 - \xi) \sum_{k=0}^{m-1} f''_{m-1-k} \frac{\partial f''_k}{\partial \xi} - \frac{\eta}{2} \sum_{k=0}^{m-1} f''_{m-1-k} f''_k \right] \quad (39)$$

with

$$\chi_m = \begin{cases} 0, & m \leq 1 \\ 1, & m > 1 \end{cases} \quad (40)$$

The general solutions $f_m(\eta, \xi)$ and $\theta_m(\eta, \xi)$ are:

$$f_m(\eta, \xi) = f_m^*(\eta, \xi) + A_1 + A_2 e^\eta + A_3 e^{-\eta} \quad (41)$$

$$\theta_m(\eta, \xi) = \theta_m^*(\eta, \xi) + A_4 e^\eta + A_5 e^{-\eta} \quad (42)$$

where $f_m^*(\eta, \xi)$ and $\theta_m^*(\eta, \xi)$ denote the special solutions in eqs. (41) and (42) and A_i ($i = 1-5$) can be determined by using the boundary conditions (37). These are:

$$A_2 = A_4 = 0, \quad A_3 = \left. \frac{\partial f_m^*(\eta, \xi)}{\partial \eta} \right|_{\eta=0}, \quad A_1 = -A_3 - f_m^*(0, \xi), \quad A_5 = -\theta_m^*(0, \xi) \quad (43)$$

Note that the problems consisting of eqs. (35)-(43) can be solved by employing the symbolic computation software MATHEMATICA for $m = 1, 2, 3, \dots$

Analysis of convergence

We notice that eqs. (33) and (34) contain the auxiliary parameters \hbar_f and \hbar_θ . These parameters can be used to adjust the convergence rate of the derived series solutions. To obtain the proper values of these parameters which give the convergent series solutions, the so called \hbar_f and \hbar_θ -curves have been plotted in figs. 1 and 2 for some fixed values of parameters. The interval on h -axis for which the \hbar_f and \hbar_θ -curves becomes parallel to the h -axis is considered to be the set of admissible values of \hbar_f and \hbar_θ . It is found that when $\xi = 0.5$ the permissible values of \hbar_f and \hbar_θ are $-1.1 \leq \hbar_f \leq -0.5$ and $-1.7 \leq \hbar_\theta \leq -0.7$, respectively. The \hbar_f -curves for different values of ξ have also been sketched. It is observed that valid range for the \hbar_f slightly shrinks with an increase in ξ . The obtained results indicate that the series solutions converge for all dimensionless time $\tau (0 \leq \tau < \infty)$ in the whole spatial domain $(0 \leq \eta < \infty)$.

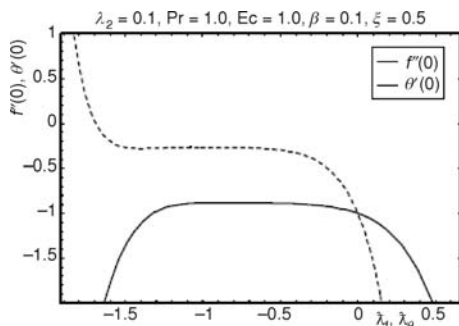


Figure 1. \hbar -curves for 15th-order of approximation

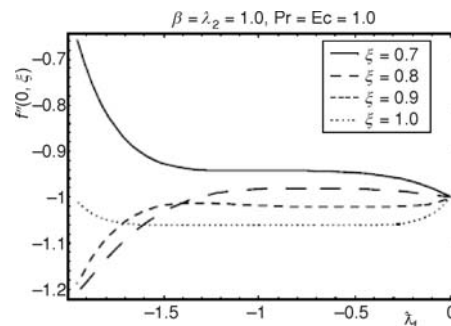


Figure 2. \hbar -curves for f for different values of ξ

Results and discussion

This section emphasizes the significance of emerging parameters on the velocity, temperature, coefficient of skin friction and local Nusselt number. It is found that when $h = -0.5$ and $\xi = 1.0$, the 5th-order homotopy solution agrees well with the exact solution, eq. (17). Furthermore, increase in the values of Deborah number β corresponds to an increase in the velocity and the boundary layer thickness. However opposite trend is noticed for the parameter λ_2 . Temperature $\theta_s(\eta)$ has been plotted vs. η for different values of η Pr and Ec. It is clear from these figs. 3 and 4 that analytic solutions obtained by HAM are in a very good agreement with the numerical solutions computed by MATHEMATICA. Figure 5 shows the behavior of dimensionless time τ

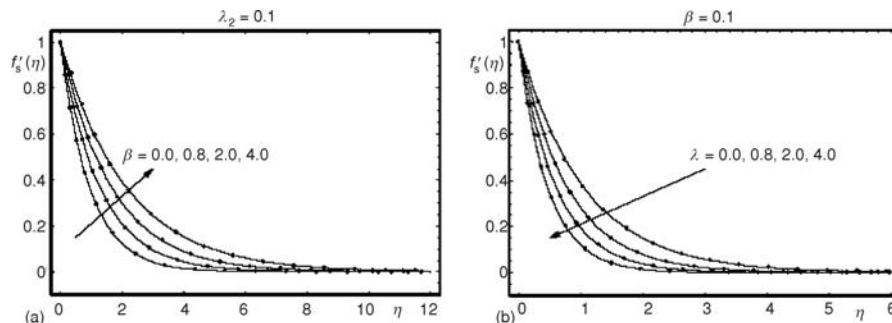


Figure 3. Velocity field $f'_s(\eta)$ for different values of β and λ_2 in the steady-state case, solid lines: exact solution eq. (17), filled circles: 15th-order homotopy solutions

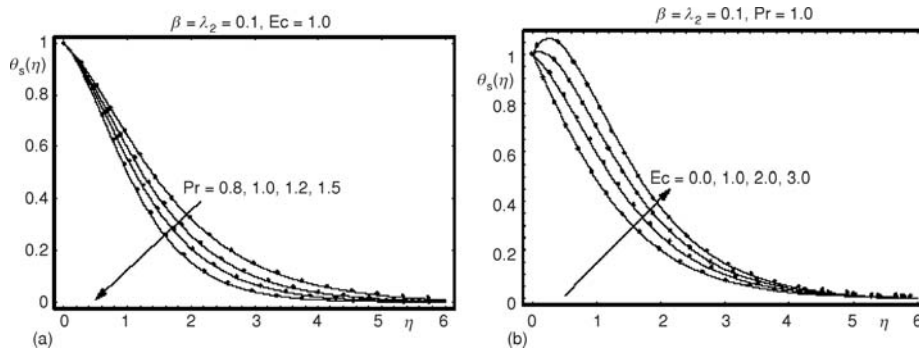


Figure 4. Temperature field $\theta_s(\eta)$ for different values of β and λ_2 in the steady-state case; solid lines: numerical solutions, filled circles: 15th-order homotopy solutions

on the velocity and the boundary layer thickness. It is seen that the velocity profiles develop rapidly from rest as τ increases until the steady-state situation ($\tau \rightarrow \infty$) is achieved. Figure 6 explores the behavior of β on the velocity field f' . Small Deborah numbers $\beta (\leq 1)$ characterize the liquid-like behavior. However the solid-like behavior is associated with large Deborah num-

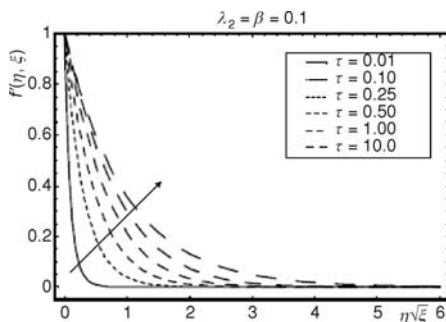


Figure 5. Influence of τ on $f'(\eta, \xi)$

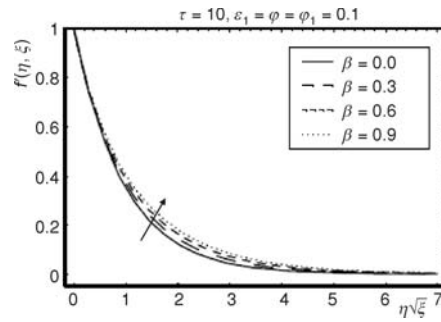


Figure 6. Effect of β on $f'(\eta, \xi)$

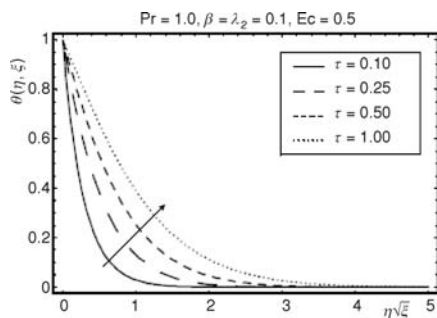


Figure 7. Effect of τ on $\theta(\eta, \xi)$

bers. Keeping this fact in mind we have only displayed the graphs for small values of Deborah number. It is observed that velocity field f' is an increasing function of β . Figure 7 examines the influence of dimensionless time τ on the temperature θ . An increase in τ corresponds to an increase in the temperature and the thermal boundary layer thickness. It is worth pointing here that temperature profiles show less deviation for large values of the time. An increase in the Prandtl number corresponds to a decrease in the temperature and the thermal boundary layer thickness. This is because for small values of the Prandtl number $Pr (< 1)$, the fluid is highly conductive. Physically, if Pr increases, the thermal diffusivity decreases and this phenomenon leads to the decreasing of energy transfer ability that reduces the thermal boundary

boundary layer thickness. This is because for small values of the Prandtl number $Pr (< 1)$, the fluid is highly conductive. Physically, if Pr increases, the thermal diffusivity decreases and this phenomenon leads to the decreasing of energy transfer ability that reduces the thermal boundary

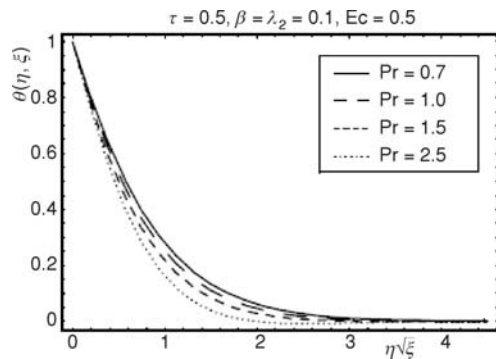


Figure 8. Effect of Pr on $\theta(\eta, \xi)$

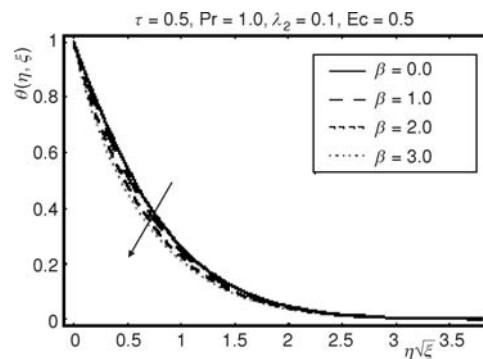


Figure 9. Effect of β on $\theta(\eta, \xi)$

layer. It is evident from fig. 9 that the outcome of an increase in β is the decay of thermal boundary layer thickness. The large values of Ec give rise to a strong viscous dissipation effect which enhances the temperature and thermal boundary layer thickness (see fig. 10).

Final remarks

The analytic solutions for momentum and heat transfer of Jeffrey fluid have been obtained. The major points can be summarized as follows.

- An increase in elastic parameter of Jeffrey fluid (the Deborah number β) corresponds to an increase in the velocity and the boundary layer thickness.
- The velocity increases and the temperature rises by increasing the dimensionless time (τ).
- The temperature and the thermal boundary layer thickness are increasing functions of Eckert number (Ec).
- Homotopy solutions are found to be in excellent agreement with the exact and numerical solutions for steady state case.

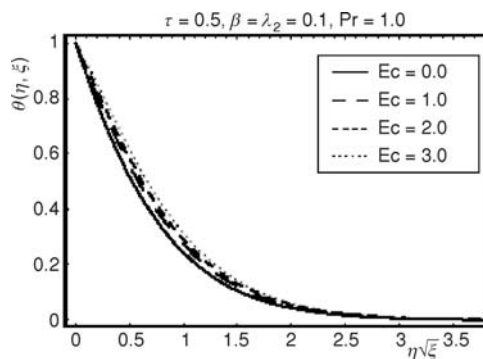


Figure 10. Effect of Ec on $\theta(\eta, \xi)$

References

- [1] Hayat, T., et al., Effects of an Endoscope and Magnetic Field on the Peristalsis Involving Jeffrey Fluid, *Comm. Nonlinear Sci. Num. Simul.* 13 (2008), 8, pp. 1581-1589
- [2] Kothandapani, M., Srinivas, S., Peristaltic Transport of a Jeffrey Fluid under the Effect of Magnetic Field in an Asymmetric Channel, *Int. J. Nonlinear Mech.* 43 (2008), 9, pp. 915-924
- [3] Hayat, T., Ali, N., Peristaltic Motion of a Jeffrey Fluid under the Effect of a Magnetic Field in a Tube, *Comm. Nonlinear Sci. Num. Simul.* 13 (2008), 7, pp. 1343-1352
- [4] Nadeem, S., Akbar, N. S., Peristaltic Flow of a Jeffrey Fluid with Variable Viscosity in an Asymmetric Channel, *Z. Naturforsch A.* 64a (2009), pp. 713-722
- [5] Crane, L. J., Flow Past a Stretching Plate, *Z. Angew. Math. Phys.*, 21 (1970), 4, pp. 645-647
- [6] Andersson, H. I., et al., Dandapat, B. S., Flow of a Power-Law Fluid Film on an Unsteady Stretching Sheet, *J. Non-Newtonian Fluid Mech.*, 62 (1996), 1, pp. 1-8
- [7] Ariel, P. D., MHD Flow of a Viscoelastic Fluid Past a Stretching Sheet with Suction, *Acta Mech.* 105 (1994), 1-4, pp. 49-56

- [8] Kumari, M., Nath, G., Analytical Solution of Unsteady Three-Dimensional MHD Boundary Layer Flow and Heat Transfer Due to Impulsively Stretched Plane Surface, *Comm. Nonlinear Sci. Num. Simul.* 14 (2009), 8, pp. 3339-3350
- [9] El-Arabawy, H. A. M., Exact Solutions of Mass Transfer over a Stretching Surface with Chemical Reaction and Suction/Injection, *J. Math. Stat.* 5 (2009), 3, pp. 159-166
- [10] Andersson, H. I., Slip Flow Past a Stretching Surface, *Acta Mech.*, 158 (2002), 1-2, pp. 121-125
- [11] Ariel, P. D., Axisymmetric Flow Due to a Stretching Sheet with Partial Slip, *Comput. Math. Appl.* 54 (2007), 7-8, pp. 1169-1183
- [12] Abbas, Z., Hayat, T., Stagnation Slip Flow and Heat Transfer over a Nonlinear Stretching Sheet, *Num. Meth. Partial Differential Equations*, 27 (2009), 2, pp. 302-314
- [13] Hayat, T., et al., Slip Flow and Heat Transfer of a Second Grade Fluid Past a Stretching Sheet through a Porous Space, *Int. J. Heat Mass Transfer*, 51 (2008), 17-18, pp. 4528-4534
- [14] Wang, C. Y., Analysis of Viscous Flow Due to a Stretching Sheet with Surface Slip and Suction, *Nonlinear Anal.: RWA.*, 10 (2009), 1, pp. 375-380
- [15] Liao, S. J., On the Analytic Solution of Magnetohydrodynamic Flows of Non-Newtonian Fluid over a Stretching Sheet, *J. Fluid Mech.*, 488 (2003), pp. 189-212
- [16] Devi, C. D. S., et al., Unsteady Mixed Convection Flow in a Stagnation Region to Adjacent to a Vertical Surface, *Heat Mass Transfer*, 26 (1991), 2, pp. 71-79
- [17] Andersson, H. I., et al., Heat Transfer in a Liquid Film on an Unsteady Stretching Surface, *Int. J. Heat Mass Transfer*, 43 (2000), 1, pp. 69-74
- [18] Nazar, R., et al., Unsteady Boundary Layer Due to a Stretching Surface in a Rotating Fluid, *Mech. Res. Comm.* 31 (2004), 1, pp. 121-128
- [19] Liao, S. J., An Analytic Solution of Unsteady Boundary-Layer Flows Caused by an Impulsively Stretching Plate, *Comm. Nonlinear Sci. Num. Simul.*, 11 (2006), 3, pp. 326-339
- [20] Mukhopadhyay, S., Effect of Thermal Radiation on Unsteady Mixed Convection Flow and Heat Transfer over a Porous Stretching Surface in a Porous Medium, *Int. J. Heat Mass Transfer*, 52 (2009), 13-14, pp. 3261-3265
- [21] Liao, S. J., On the Relationship between the Homotopy Analysis Method and Euler Transform, *Comm. Nonlinear Sci. Numer. Simul.*, 15 (2010), 6, pp. 1421-1431
- [22] Liao, S. J., Notes on the Homotopy Analysis Method: Some Definitions and Theorems, *Comm. Non-linear Sci. Num. Simul.* 14 (2009), 4, pp. 983-997
- [23] Abbasbandy, S., Shivanian, E., Prediction of Multiplicity of Solutions of Nonlinear Boundary Value Problems: Novel Application of Homotopy Analysis Method, *Comm. Nonlinear Sci. Num. Simul.*, 15 (2010), 12, pp. 3830-3846
- [24] Abbasbandy, S., Shirzadi, A., A New Application of the Homotopy Analysis Method: Solving the Sturm-Liouville Problems, *Comm. Nonlinear Sci. Num. Simul.*, 16 (2011), 1, pp. 112-126
- [25] Rashidi, M. M., Mohimaniyan Pour, S. A., Analytic Approximate Solutions for Unsteady Boundary-Layer Flow and Heat Transfer Due to a Stretching Sheet by Homotopy Analysis Method, *Nonlinear Analysis: Modelling and Control*, 15 (2010), 1, pp. 83-95
- [26] Bataineh, A. S., et al., On a New Reliable Modification of Homotopy Analysis Method, *Comm. Nonlinear Sci. Num. Simul.*, 14 (2009), 2, pp. 409-423
- [27] Hayat, T., et al., Soret and Dufour Effects on the Stagnation-Point Flow of a Micropolar Fluid toward a Stretching Sheet, *ASME-J. Fluids Eng.*, 133 (2011), 2, pp. 021202
- [28] Hayat, T., et al., Unsteady Flow with Heat and Mass Transfer of a Third Grade Fluid over a Stretching Surface in the Presence of Chemical Reaction, *Non-Linear Anal. RWA.*, 11 (2010), 4, pp. 3186-3197
- [29] Hayat, T., et al., Time-Dependent Three-Dimensional Flow and Mass Transfer of Elastico-Viscous Fluid over Unsteady Stretching Sheet, *Appl. Math. Mech.*, 32 (2011), 2, pp. 167-178
- [30] Hayat, T., et al., Melting Heat Transfer in the Stagnation-Point Flow of an Upper-Convected Maxwell (UCM) Fluid Past a Stretching Sheet, *Int. J. Num. Meth. Fluids.*, 68 (2012), 2, pp. 233-243

Paper submitted: September 7, 2011

Paper revised: April 28, 2012

Paper accepted: May 8, 2012